Maternal inflammation promotes fetal microglial activation and increased cholinergic expression in the fetal basal forebrain: role of interleukin-6

Lorelei Pratt[1], Li Ni[2], Nicholas M. Ponzio[3] and G. Miller Jonakait[2]

BACKGROUND: Perinatal exposure to infectious agents with associated maternal immune activation (MIA) leads to neuroanatomical and behavioral dysregulation reminiscent of autism spectrum disorders. Persistent microglial activation as well as increased choline acetyltransferase (ChAT) activity in the basal forebrain (BF) are characteristic of autistic subjects. Previous studies have shown that medium from activated microglia promotes cholinergic differentiation of precursors in the BF. We sought to determine whether MIA *in vivo* would lead to a similar effect on developing BF neurons.

METHODS: Pregnant mice were treated with the viral mimic polyinosinic–polycytidylic acid (poly(I:C)) or saline.

RESULTS: Poly(I:C) treatment resulted in increased production of cytokines and chemokines in fetal microglia and increased ChAT activity and cholinergic cell number in the perinatal BF. Whether microglial activation causes these changes is unclear. Examination of fetal brains from mice lacking interleukin-6 (IL-6 KOs) revealed an elevation in non–microglial-derived cytokines and chemokines over wild-type controls. Moreover, IL-6 KO offspring showed an elevation of ChAT activity even in the absence of poly(I:C) administration.

CONCLUSION: These data suggest that elevations in cytokines and/or chemokines caused either by maternal poly(I:C) administration or by the absence of IL-6 are associated with alterations in cholinergic development in the BF.

The causes of autism spectrum disorders remain unclear. Recent papers describing possible genetic bases for autism spectrum disorder have been promising (1,2), but evidence also suggests that perinatal exposure to infectious agents with associated maternal and/or fetal immune activation may combine with a genetic predisposition to produce autism spectrum disorder and schizophrenia (3–8). Animal studies confirm that maternal immune activation (MIA) leads to behavioral and morphological anomalies reminiscent of the disorder (9–13). Although mechanisms remain unclear, fetal microglia may be involved.

Microglia appear in the fetal brain at about embryonic day (E)11–E12 in the rat (14). When activated *in vitro* by inflammatory cytokines and Toll-like receptor ligands such as lipopolysaccharide, peptidoglycan, and/or polyinosinic–polycytidylic acid (poly(I:C)), they increase the production of reactive oxygen species and produce proinflammatory chemokines and cytokines that can be toxic to mature neurons and oligodendrocytes. Of note for the study of autism, brains of autistic subjects show evidence of persistent microglial activation (15–17).

Effects of microglial activation on embryonic systems have been studied rarely and almost exclusively in culture. Studies from our laboratory and those of others have shown that a cocktail of factors released from stimulated microglia induces cholinergic differentiation of undifferentiated precursors from the mid-gestational basal forebrain (BF) (18–20). Moreover, activity of choline acetyltransferase (ChAT), the hallmark of cholinergic neurons, is elevated in the BFs of autistic subjects (21), and post-mortem analysis reveals an increased number and an enlargement of cholinergic BF neurons in autistic children (22). It is not certain, however, that MIA leads to changes in fetal microglial cytokine production, or that cholinergic development in the BF *in vivo* is affected. These aspects of MIA are investigated here.

RESULTS

Culture studies have demonstrated that factors produced by activated microglia promote cholinergic differentiation of undifferentiated embryonic BF precursor cells (18–20). Whether MIA results in increased ChAT activity or increased numbers of cholinergic neurons in the fetal BF *in vivo* has not been investigated. To address this question, pregnant mice at embryonic day (E)12.5 were injected with poly(I:C) or sterile saline, and the BFs of their embryos/offspring were assayed for ChAT activity and assessed by stereology for numbers of ChAT+ neurons.

Poly(I:C) Treatment Affects Behavior and Weight Gain of Dams

To verify the effectiveness of the poly(I:C) injection, maternal weight and behavior were monitored. Control females injected

[1]Department of Biological Sciences, Rutgers University, Newark, New Jersey; [2]Department of Biological Sciences, New Jersey Institute of Technology, Newark, New Jersey; [3]Department of Pathology and Laboratory Medicine, New Jersey Medical School, University of Medicine and Dentistry, Newark, New Jersey. Correspondence: Lorelei Pratt (lpratt@andromeda.rutgers.edu)

Received 18 December 2012; accepted 2 April 2013; advance online publication 7 August 2013. doi:10.1038/pr.2013.126

with saline showed an average gain of +0.64 ± 0.08 g (n = 51) 24 h after injection. By contrast, poly(I:C)-injected females showed a significant loss of −0.91 ± 0.12 g (n = 66; P < 0.001).

Sickness behavior was also assessed. Four hours after injection, saline-injected animals received a total score of 19.3 ± 0.19 (n = 41), indicating normal behavior. All dams were active, exploring and responsive in a novel environment. By contrast, poly(I:C)-injected dams were lethargic and unresponsive, scoring only 6.03 ± 0.75 (n = 54; P < 0.0001). However, after 24 h, all females exhibited normal behavior. The loss-of-weight and behavioral assessments indicate that poly(I:C) injection causes a robust but transient response.

Poly(I:C) administration did not affect the length of gestation, number of pups, nor crown-to-rump lengths of embryos (data not shown).

Poly(I:C) Treatment Results in an Increase in ChAT Activity in the BF

To determine ChAT activity in the fetal BFs following MIA, BFs were dissected from E16.5 and E18.5 embryos and postnatal day (P)1 pups and assayed. ChAT activity was significantly higher following poly(I:C) treatment at these time points (Figure 1a). Data using all individual BF samples as separate data points also revealed a significant difference between the two groups (Figure 1b; P < 0.0001). By P9, however, ChAT levels were indistinguishable between the groups (Figure 1c), demonstrating that cholinergic activity increases transiently in the fetal BF following MIA.

Poly(I:C) Treatment Produces an Increased Number of Cholinergic Neurons in the BF

To determine whether the number of cholinergic neurons in the fetal BF also increases *in vivo* following MIA, transgenic mice that express enhanced green fluorescent protein (EGFP) under the control of the ChAT promoter were used. At E12.5, pregnant mice were injected with either saline or poly(I:C), and stereology was performed to obtain an estimate of the number of cholinergic neurons at E16.5 and P1.

The number of cholinergic neurons was significantly higher at E16.5 and at P1 in the poly(I:C) group as compared with controls (Figure 2). At E16.5, the average estimated number of ChAT+ neurons increased from 1,869 ± 111 in the control samples to 3,336 ± 451 in the poly(I:C) samples. At P1, there was also an increase in the number of ChAT+ neurons from 10,354 ± 497 in the control group to 17,770 ± 616 in the poly(I:C) group. These findings are consistent with the increase in ChAT activity observed in early BF development and suggest that MIA has a marked effect on cholinergic development in the fetal BF.

Poly(I:C) Treatment Affects Glutamic Acid Decarboxylase Activity in the BF

In BF cultures, an increase in ChAT activity and cholinergic cell number is accompanied by a decrease in message for glutamic acid decarboxylase (GAD)65 (20). To determine whether a similar reduction occurs *in vivo*, RNA was extracted from

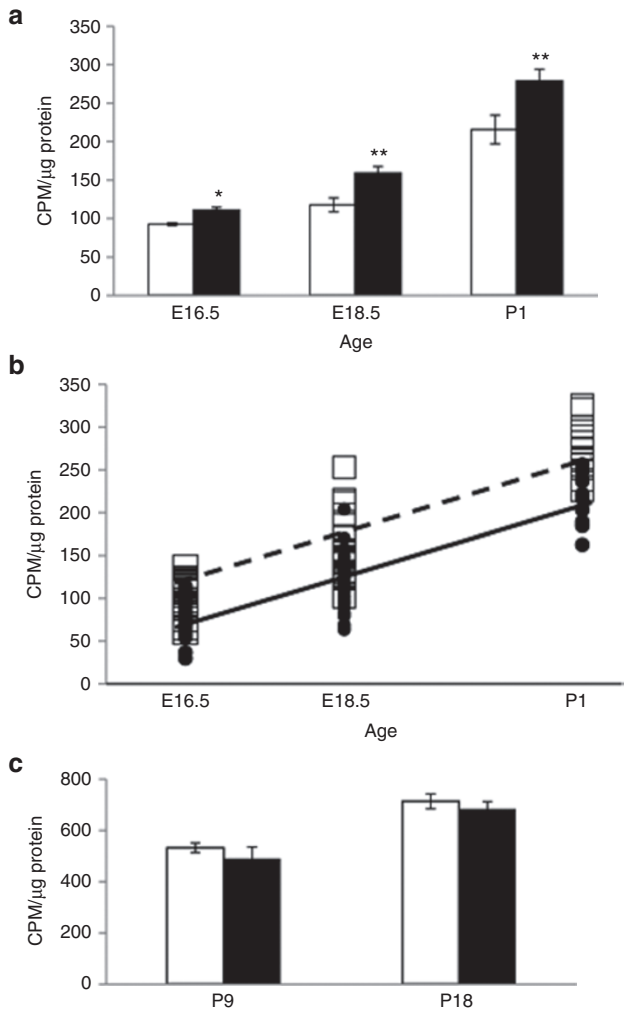

Figure 1. ChAT activity in the fetal basal forebrain increases following maternal poly(I:C) injection. ChAT activity was measured in basal forebrains (BFs) taken from (**a,b**) E16.5, E18.5, and P1, as well as (**c**) P9 and P18 BFs of offspring of saline- and poly(I:C)-injected mice. Data are expressed as CPM of acetylcholine formed/µg protein in the sample. The average CPM/µg protein for all BFs from a single litter was considered an n of 1 (**a** and **c**). Data were compared using a two-way ANOVA with a *post hoc* Tukey test (n = 4 litters per treatment; *P < 0.05, **P < 0.01). In (**a**) and (**c**), white bars are controls; black bars are poly(I:C)-treated samples. (**b**) BF samples were considered individually and analyzed with an ANCOVA and a *post hoc* Tukey test to compare ChAT activity between treatment groups while taking into account the effect of time (P < 0.0001; control: n = 69; poly(I:C): n = 61; R^2 = 0.777). Solid line indicates the model for controls; the dashed line indicates the model for poly(I:C)-treated samples. ANCOVA, analysis of covariance; ChAT, choline acetyltransferase; CPM, counts per minute; E, embryonic day; P, postnatal day; poly(I:C), polyinosinic–polycytidylic acid.

E16.5 and P1 BFs of offspring of both saline- and poly(I:C)-injected mice. Message levels for GAD65 and the related molecules GAD67 and gamma-aminobutyric acid receptor α-subunit 1 (GABARα1)were quantified by quantitative real-time PCR (qRT-PCR). Message for GAD65 was significantly lower in the E16.5 BFs of embryos of poly(I:C)-treated dams (Figure 3). No significant differences were found in expression levels of GAD67 or GABARα1. At P1, none of the molecules was significantly different from that of the control.

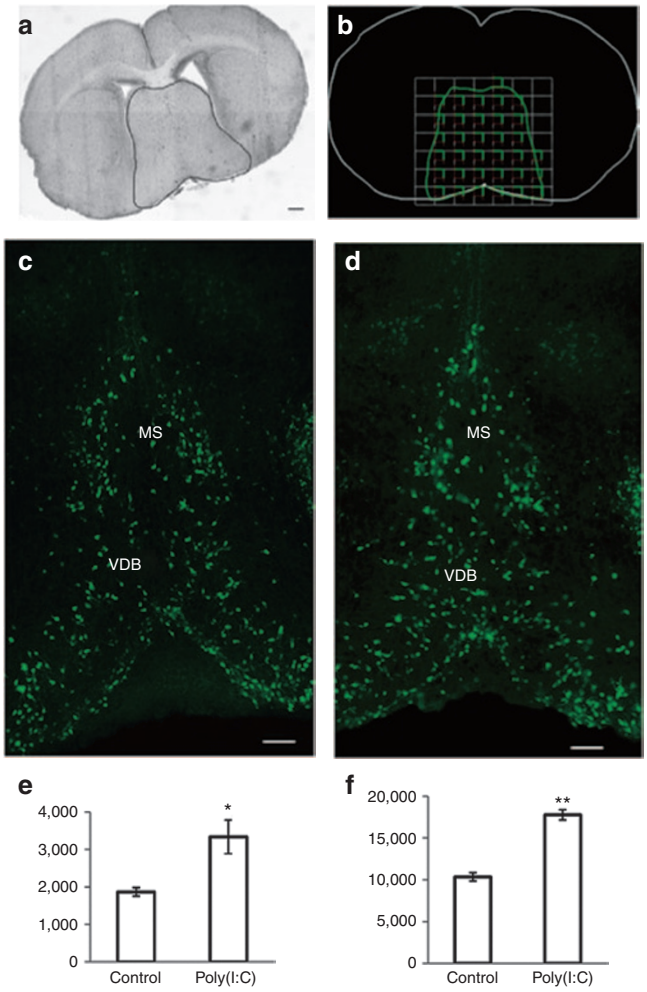

Figure 2. The number of cholinergic neurons in the fetal basal forebrain increases following maternal immune activation. Coronal brain sections (60 µm) from E16.5 and P1 offspring of saline- and poly(I:C)-injected ChAT-EGFP mice were prepared for stereological analysis of cholinergic population size (see Methods section). (**a**) P1 coronal section with BF region outlined indicating the area in which ChAT+ cells were counted. Scale bar = 250 µm. (**b**) P1 section showing grid overlay on BF region with systematic placement of counting frames. (**c,d**) Micrographs showing ChAT-EGFP expression in the BFs of P1 brains from (**c**) control and (**d**) poly(I:C) treatment groups. Scale bar = 100 µm.. (**e,f**) Population estimates at (**e**) E16.5 and (**f**) P1 compared using Student's *t*-test. Estimates from brains of a single litter were averaged and considered an *n* of 1. Sections were sampled from a 600-µm portion of E16.5 BFs (**P* = 0.034; *n* = 3) and a 720-µm portion of P1 BFs (***P* < 0.001; *n* = 3). BF, basal forebrain; ChAT, choline acetyltransferase; E, embryonic day; EGFP, enhanced green fluorescent protein; MS, medial septum; P, postnatal day; poly(I:C), polyinosinic–polycytidylic acid; VDB, vertical diagonal band.

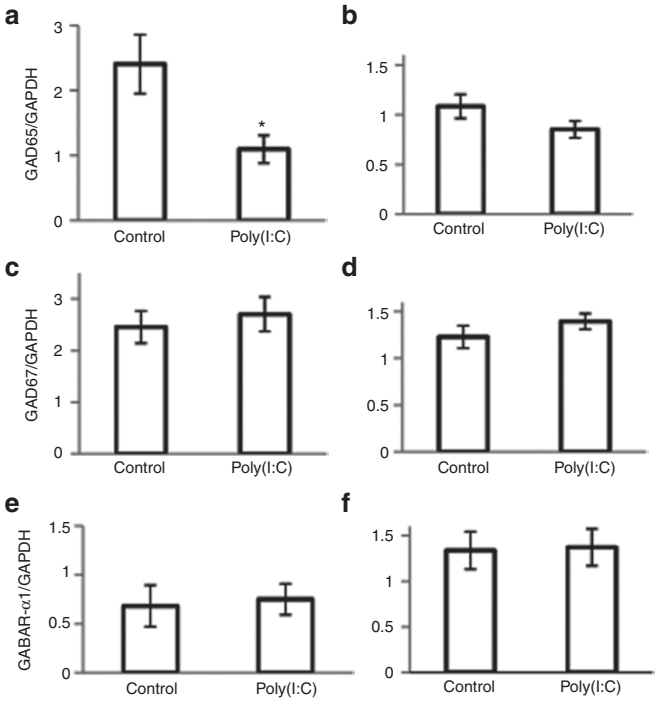

Figure 3. GAD65 mRNA decreases in the E16.5 fetal basal forebrain following poly(I:C) injection. RNA was extracted from the BFs of (**a,c,e**) E16.5 and (**b,d,f**) P1 offspring of saline- and poly(I:C)-injected mice. Levels of (**a,b**) GAD65, (**c,d**) GAD67, and (**e,f**) the α-subunit 1 of the GABA receptor (GABARα1) were determined by qRT-PCR. Expression levels were normalized to GAPDH, and ratios expressed as arbitrary units. Data were compared using Student's *t*-test. (**a**) **P* = 0.031, *n* = 5 for each group. (**b,d,f**) *n* = 3. (**c,e**) *n* = 5. Average for each litter is considered as an *n* of 1. BF, basal forebrain; E, embryonic day; GABA, gamma-aminobutyric acid; GAD, glutamic acid decarboxylase; GAPDH, glyceraldehyde 3-phosphate dehydrogenase; P, postnatal day; poly(I:C), polyinosinic–polycytidylic acid; qRT-PCR, quantitative real-time PCR.

Fetal Microglia Are Activated by MIA

Finding these changes in the embryonic BF *in vivo* raised the question of whether activated fetal microglia were responsible for those changes. Pregnant mice were injected with poly(I:C) or sterile saline at E12.5. At E16, fetal brains were prepared either for qRT-PCR analysis or the Luminex assay (EMD Millipore, Billerica, MA). Although other studies have shown that levels of inflammatory cytokines rise within the fetal brain following a maternal immune challenge (9,23,24), direct demonstration that microglia are the source of these cytokines is lacking (however, see refs. 25 and 26).

An enriched fraction of $CD11b^+$ cells (microglia) was prepared for qRT-PCR analysis of proinflammatory cytokines interleukin (IL-)1β, IL-6, and tumor necrosis factor-α, as well as the anti-inflammatory IL-10. Of the three proinflammatory mediators assessed, only IL-6 showed a significant increase following MIA (Figure 4a).

To assess protein production of a broader array of cytokines and chemokines, a 32-plex Luminex assay was used. An enriched population of E16.5 $CD11b^+$ fetal microglia was obtained (~10^6 cells) for each of three experiments.

Consistent with mRNA data, neither tumor necrosis factor-α nor IL-1β showed an increase following MIA. Although the mRNA for IL-6 had increased, the IL-6 protein levels failed to reach statistical significance in the Luminex assay, although the trend was upward. Of the classic proinflammatory cytokines, IL-1α was significantly elevated. Other cytokines showing significant elevations included granulocyte-macrophage/monocyte colony-stimulating factor, macrophage/monocyte colony-stimulating factor, IL-4, and IL-9 (Figure 4b).

Unexpectedly, a number of chemokines also showed statistically significant increases, including eotaxin, macrophage

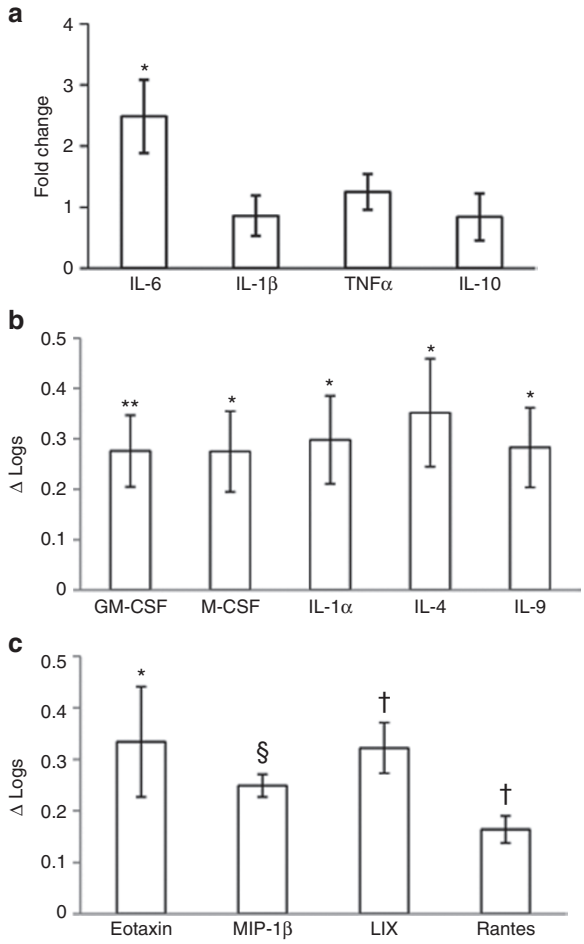

Figure 4. Fetal microglia express altered cytokine and chemokine levels following MIA. Pregnant mice were injected at E12.5 with poly(I:C) (20 mg/kg) or sterile saline, and fetal brains from an entire litter were collected at E16.5. An enriched population of $CD11b^+$ (i.e., microglial) cells was obtained using magnetic beads (Methods section). (**a**) qRT-PCR was performed and cytokine expression levels were normalized to GAPDH. Data are expressed as fold change (poly(I:C)-treated over control). Data for each cytokine were compared for significance using a single-sample one-tailed *t*-test (*$P = 0.04$; $n = 4$ litters). (**b,c**) $CD11b^+$ lysates were assayed for protein expression using a Luminex 32-plex mouse cytokine/chemokine assay. The assay was conducted three times on six litter samples. Data were expressed as pg/mg protein. For comparison across assays, these numbers were log transformed, and the difference between logs was assessed using a single-sample one-tailed *t*-test. Data are presented as the average difference in logs ± SEM for (**b**) cytokines and (**c**) chemokines that were significantly upregulated in the $CD11b^+$ poly(I:C) treatment group. *$P = 0.04$; **$P = 0.03$; §$P = 0.004$; †$P = 0.01$. E, embryonic day; GAPDH, glyceraldehyde 3-phosphate dehydrogenase; GM-CSF, granulocyte-macrophage colony-stimulating factor; LIX, lipopolysaccharide-induced CXC chemokine; M-CSF, macrophage colony-stimulating factor; MIP-1β, macrophage inflammatory protein 1β; MIA, maternal immune activation; poly(I:C), polyinosinic–polycytidylic acid; qRT-PCR, quantitative real-time PCR; Rantes, regulated upon normal T cell expressed and secreted.

inflammatory protein 1β, lipopolysaccharide-induced CXC chemokine, and regulated upon activation normal T cell expressed and secreted (RANTES). Monocyte chemoattractant protein 1, although not reaching statistical significance, also trended upward (Figure 4c).

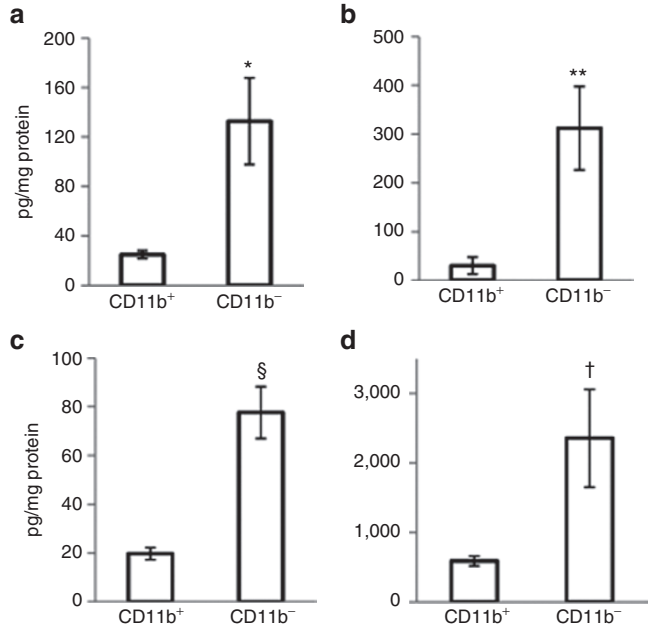

Figure 5. Nonmicroglial cells produce cytokines. Pregnant WT mice were injected at E12.5 with poly(I:C) (20 mg/kg) or saline (CT), and fetal brains from an entire litter were collected at E16.5. After magnetic bead separation, protein was extracted from both the enriched $CD11b^+$ population (i.e., microglial cells) and the $CD11b^-$ population (i.e., all other fetal brain cells). Cells were separated on three different occasions from six separate litters. The Luminex 32-plex assay was conducted three times. Data from microglial fractions and nonmicroglial fractions were pooled disregarding treatment. The data are expressed as pg/mg protein and were compared for significance using Student's *t*-test. (**a**) IL-1β, *$P = 0.001$; (**b**) IL-9, **$P = 0.047$; (**c**) IL-10, §$P = 0.0009$; (**d**) IL-13, †$P = 0.004$. $n = 6$ litters for all groups. E, embryonic day; IL, interleukin; poly(I:C), polyinosinic–polycytidylic acid; WT, wild type.

Although our focus was on $CD11b^+$ (i.e., microglial) fractions, the $CD11b^-$ fractions also produced significant quantities of cytokines following maternal inflammation, often in larger quantities than the $CD11b^+$ fractions. These included IL-1β, IL-9, IL-10, and IL-13 (Figure 5). These data confirm that microglia are activated following maternal injection with poly(I:C) and that fetal brain cells other than microglia are producing cytokines.

To determine whether maternal immune challenge resulted in an increased number of microglia, microglia were assessed by stereology in the brains of embryos of both saline- and poly (I:C)-injected CX3CR1-EGFP mice. There was no significant difference in population estimates between control and poly(I:C) groups. Average microglial population estimates were 3,887 ± 353 for the controls and 3,800 ± 479 for the poly(I:C) group at E16.5 and 9,156 ± 933 and 9,381 ± 719, respectively, at P1 for the same two groups.

The Role of IL-6

The increase in IL-6 mRNA as well as reports from other studies that IL-6 is a mediator of fetal brain dysregulation following MIA (27) prompted us to determine whether IL-6 plays a role in altering cholinergic expression after poly(I:C) injection using mice lacking IL-6 (IL-6 KO). BFs were dissected from E16.5 and E18.5 embryos and P1

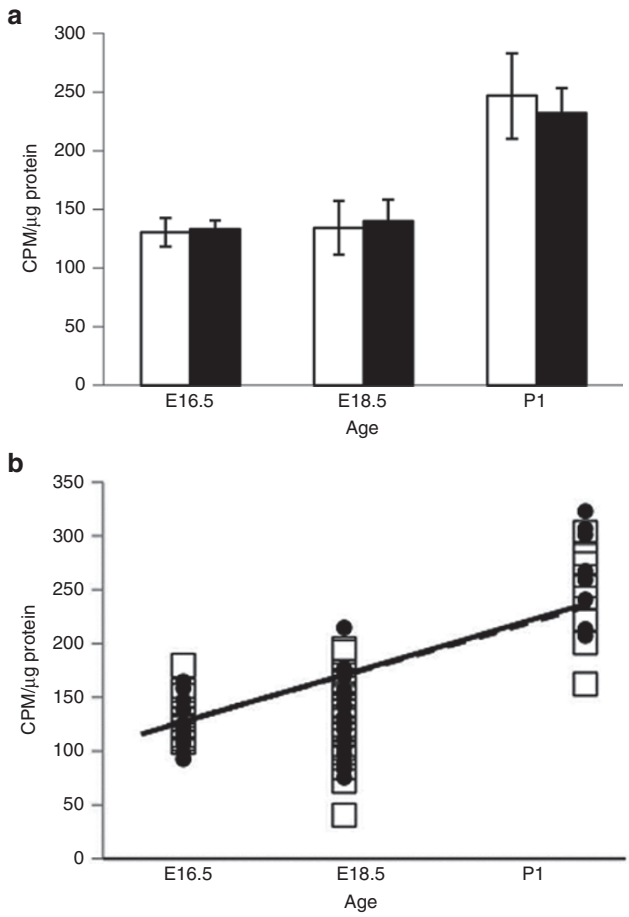

Figure 6. ChAT activity in the IL-6 KO fetal basal forebrain does not change following maternal poly(I:C) injection. ChAT activity was measured in BFs taken from (**a,b**) E16.5, E18.5, and P1 offspring of saline- and poly(I:C)-injected IL-6 KO mice. Data are expressed as CPM/µg protein. (**a**) The average of BFs from each litter was considered an *n* of 1. Data were compared using a two-way ANOVA. $P = 0.917$, $n = 2$ litters for each treatment group at E16.5 and P1. At E18.5, $n = 3$ litters for control and $n = 4$ litters for the poly(I:C) group. White bars indicate IL-6 KO control; black bars indicate IL-6 KO poly(I:C)-treated mice. (**b**) BF samples were considered individually and analyzed with an ANCOVA to compare ChAT activity between treatment groups while taking into account the effect of time ($P = 0.984$; control: $n = 40$; poly(I:C): $n = 43$; $R^2 = 0.509$). Solid line indicates the model for control; dashed line indicates the model for poly(I:C)-treated samples. ANCOVA, analysis of covariance; BF, basal forebrain; ChAT, choline acetyltransferase; CPM, counts per minute; E, embryonic day; IL-6 KO, mice lacking interleukin-6; P, postnatal day; poly(I:C), polyinosinic–polycytidylic acid.

pups of wild-type (WT) and IL-6 KO females injected with poly(I:C) or saline and assayed for ChAT activity. Unlike the WT (see above; **Figure 1**), there was no significant difference in ChAT activity between saline- and poly(I:C)-treated KO mice (**Figure 6a**). An analysis of covariance revealed that data from both the groups are represented by a single line with no significant difference due to treatment (**Figure 6b**). This is unlike the WT mice, for which the data are best represented as two separate linear relationships both dependent on time but with the poly(I:C) group producing more counts per minute (CPM)/µg protein at each time point (**Figure 1b**).

The Absence of IL-6 Promotes an Inflamed Fetal Brain Environment

$CD11b^+$ and $CD11b^-$ fractions from E16.5 embryonic brains of both WT and IL-6 KOs were analyzed by Luminex. Cytokine and chemokine production was first evaluated in $CD11b^+$ fractions from saline-treated dams. When $CD11b^+$ samples from saline-injected WT embryos were compared with saline-injected IL-6 KOs, no significant differences were detected. However, comparisons of the poly(I:C)-treated WT mice with the poly(I:C)-treated KOs revealed a major change. In the WT animals in the $CD11b^+$ fraction, poly(I:C) elevates IL-1α, IL-4, IL-9, granulocyte-macrophage/monocyte colony-stimulating factor, macrophage/monocyte colony-stimulating factor, eotaxin, macrophage inflammatory protein 1β, lipopolysaccharide-induced CXC chemokine, and regulated upon activation normal T cell expressed and secreted (RANTES) (see above). However, in the KO animals, these statistically significant increases did not occur. These data suggest a possible role for IL-6 in regulating microglial output of cytokines and chemokines, both in normal development as well as in response to MIA.

The $CD11b^-$ fractions also show differences between WT and IL-6 KO animals. When saline-treated WT animals were compared with saline-treated KOs, interferon γ, monocyte induced by interferon γ, IL-9, IL-10, IL-12p70, IL-13, monocyte chemoattractant protein 1, macrophage inflammatory protein 1α, and regulated upon activation normal T cell expressed and secreted (RANTES) were all significantly elevated in the KOs (**Figures 7a,b**). Therefore, data from the $CD11b^-$ fractions indicate an altered fetal brain environment at E16.5 that is not associated with maternal poly(I:C) injection but due simply to the absence of IL-6. It appears, therefore, that the absence of IL-6 alters the fetal brain environment toward a more inflammatory phenotype. These data point to a broad role for IL-6 in maintaining immunological homeostasis in the fetal brain. Because the brain environment is already inflamed in KOs, maternal poly(I:C) injection may not elevate levels further. This is consistent with the data of Lasala *et al.* (28), who have suggested that a preexisting inflammatory environment may suppress a subsequent response to inflammation.

IL-6 KOs Show Elevated Levels of ChAT in the BF

A significant difference also emerged when ChAT activity in the BF was examined. There were no differences between the levels of ChAT in the saline-treated KOs as compared with the poly(I:C)-treated KOs at E16.5, E18.5, and P1. However, at E16.5, the levels of ChAT in both saline-treated KOs and poly(I:C)-treated KOs were higher than those of the poly(I:C)-treated WT mice (**Figure 7c**). It appears, then, that the mere absence of IL-6 produces a fetal brain inflammatory environment not unlike the poly(I:C) injection in WT mice and results in an effect on BF cholinergic neurons that is similar. This is reflected as well in GAD65 expression. In the WT mice, poly(I:C) injection results in a decrease in GAD65 mRNA at E16.5 (**Figure 3**). However, both the saline-injected and poly(I:C)-injected KOs show a downregulation of GAD65

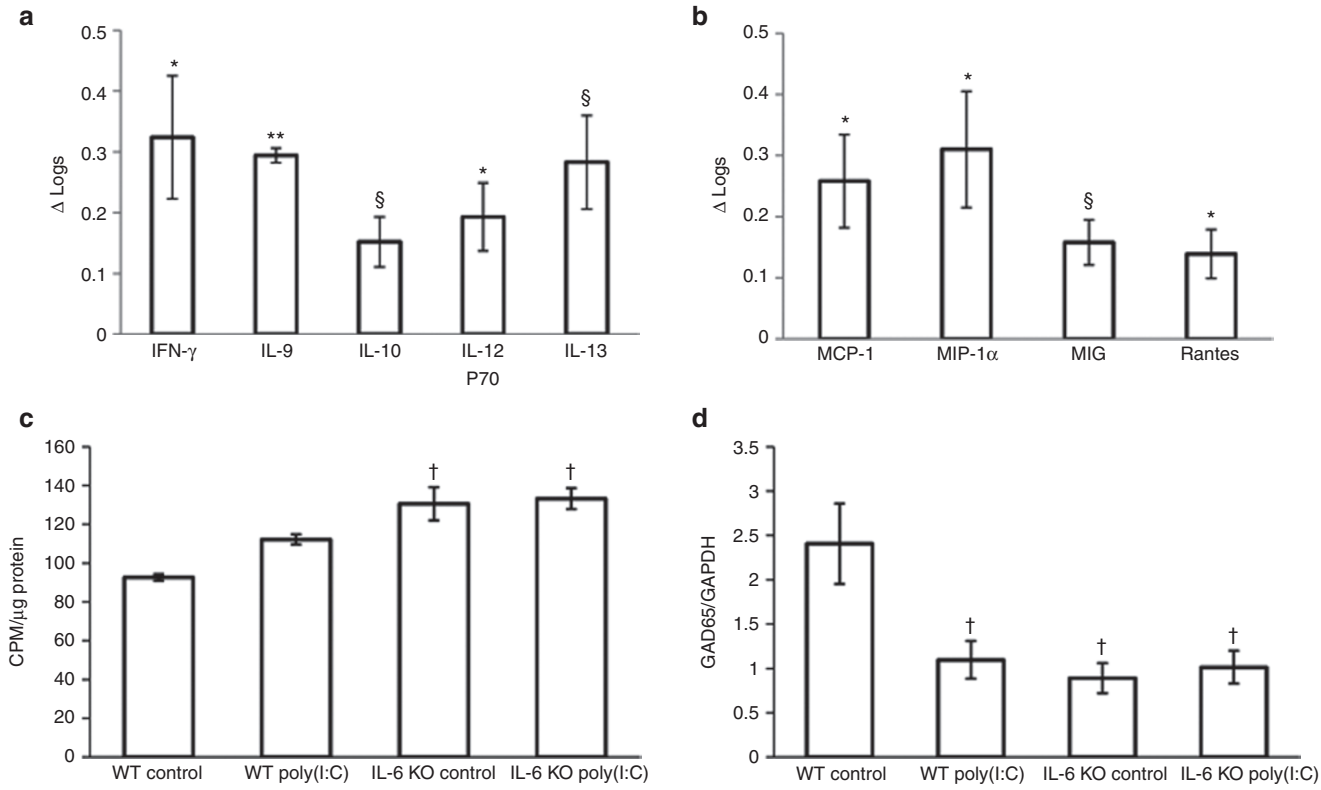

Figure 7. The fetal brain cytokine/chemokine environment is altered in IL-6 KOs. Pregnant WT and IL-6 KO mice were injected at E12.5 with sterile saline, and (**a,b**) fetal brains from an entire litter were collected at E16.5. $CD11b^-$ lysates were assayed for protein expression using a Luminex assay. The assay was conducted three times on three different samples from each of the treatment groups. Data were normalized to the amount of protein in each sample and expressed as the log of pg/mg protein. Data are presented as the average difference in logs ± SEM for (**a**) cytokines and (**b**) chemokines that were significantly upregulated in the $CD11b^-$ KO mice. The difference between logs was assessed using a single-sample one-tailed *t*-test. $^*P = 0.04$; $^{**}P = 0.02$; $^{\S}P = 0.03$. (**c**) ChAT activity (CPM/μg protein) was assessed in E16.5 BFs taken from WT saline- or poly(I:C)-treated dams and from IL-6 KOs treated with saline or poly(I:C). The average of BFs from each litter was considered an *n* of 1. Data were compared using a two-way ANOVA with poly(I:C) and the absence of IL-6 as the two treatment factors. A *post hoc* Tukey test was used to determine significance. IL-6 KO BF samples show significantly higher ChAT activity than WT mice ($^{\dagger}P < 0.01$; $n = 4$ for control, $n = 2$ for IL-6 KO). There is no significant difference in ChAT activity due to poly(I:C) treatment within the IL-6 KO group. (**d**) qRT-PCR was performed to determine GAD65 expression in BFs of E16.5 embryos from saline- or poly(I:C)-injected WT and IL-6 mice. Data were normalized to GAPDH, and the ratio expressed as arbitrary units. Data are compared using a two-way ANOVA and *post hoc* Tukey test. No significant difference is found in mRNA expression between control and poly(I:C) treatments within the IL-6 KO group. IL-6 KO GAD65 message levels are lower than those in WT controls and are not significantly different from WT poly(I:C) levels. $^{\dagger}P < 0.01$; $n = 5$ litters for WT and IL-6 KO poly(I:C) samples; $n = 3$ litters for IL-6 KO control). BF, basal forebrain; ChAT, choline acetyltransferase; CPM, counts per minute; E, embryonic day; GAD65, glutamic acid decarboxylase 65; GAPDH, glyceraldehyde 3-phosphate dehydrogenase; IL-6 KO, mice lacking interleukin-6; poly(I:C), polyinosinic–polycytidylic acid; qRT-PCR, quantitative real-time PCR; WT, wild type.

similar to that seen with poly(I:C) in WT animals (Figure 7d). Therefore, in the BF, the absence of IL-6 produces effects that are similar to those of poly(I:C) injection.

DISCUSSION

The use of poly(I:C) as a viral mimic to induce maternal infection in animal studies is now well established. Moreover, the evidence suggesting that MIA adversely affects fetal brain development is not in dispute. Whether MIA in general and poly(I:C) injection in particular serve as accurate animal models for autism spectrum disorders is, however, not at all certain. We have used it here as a useful, replicable model of MIA.

Using the 32-plex Luminex assay, we have shown that fetal microglia respond to this stimulus with the upregulation of several cytokines and chemokines. Certain limitations are inherent in this assay. To obtain sufficient numbers of fetal cells for the assay, enriched microglial samples were extracted from whole fetal brains. Therefore, our results do not reflect regional differences that may occur. Recent studies have revealed evidence for differences in cytokine/chemokine expression by region in postnatal brain tissue analysis following MIA (29). These postnatal differences may be indicative of prenatal variation by region as well. Other canonical indications of microglial activation were not observed. So, for example, we did not detect increased numbers of microglia in the poly(I:C)-treated embryos, suggesting that proliferation was not enhanced. Nor did we see retraction of microglial processes and changes in soma size (data not shown). Having found, however, that fetal brains respond to maternal poly(I:C) injection, we were eager to explore the effects of MIA on cholinergic development in the BF.

Fetal ChAT Activity and Cholinergic Cell Number Increase Following MIA

Original studies indicated that activated microglia produce factors that promote cholinergic differentiation of undifferentiated precursors in the cultured embryonic BF (19,20,30).

These findings in culture were intriguing given the facts that activated microglia persist in autistic subjects (15), that ChAT activity is elevated in the BFs of autistic brains (21), and that BF neurons in autistic children are enlarged and more plentiful than in normal subjects (22). Our findings now show an increase in both the number of cholinergic neurons and ChAT activity in the fetal/perinatal BF *in vivo* following MIA. Although we have found an association between microglial cytokine production and increased cholinergic activity in the BF, whether changes in the BF are a direct result of that microglial activation remains unclear.

Similar to findings in culture, GAD65 levels in the BF declined as ChAT activity increased. The transient decrease in GAD65 expression could reflect a delay or a skewing in the differentiation of GABAergic interneurons. Because of the variety of GABAergic interneurons that are derived from temporally separated progenitor pools, the normal differentiation and/or distribution of these pools may have been affected (31).

Role of IL-6

IL-6 has assumed particular significance in the autism literature both because it is elevated in the brains of autistic patients (15) and because it has been touted as a mediator of MIA's effects on the fetal brain (27). These suggestions are buttressed by studies showing behavioral and cognitive abnormalities in adult mice following prenatal injection of IL-6 (27,32,33). A maternal immune response includes placental production of IL-6 (34,35), and that production is greatly increased following MIA (34,36). Although we and others show fetal brain increases in IL-6 mRNA following MIA (24), the Luminex assay did not reveal increased IL-6 protein. However, because our assay was performed 4 d after poly(I:C) injection, we may have missed an acute response that included increased IL-6 expression.

Although it is unclear whether IL-6 is produced in significant quantities within the fetal brain following MIA, our findings shed light on additional aspects of IL-6 function in the developing brain. In our experiments, offspring of saline-injected IL-6 KO mice had increased levels of inflammatory cytokines and chemokines in the $CD11b^-$ fractions as compared with offspring of WT, saline-injected mice. Therefore, the embryonic brain environment in the KOs is inflamed without ever being exposed to poly(I:C). Moreover, in the WT fetal brain, $CD11b^+$ cells produce a robust reaction to the poly(I:C) immune challenge. However, no such reaction is apparent in the IL-6 KO mice. Therefore, in the KOs, no significant difference in cytokine/chemokine production was found between the saline and poly(I:C) treatment groups in either the $CD11b^+$ or the $CD11b^-$ fractions, suggesting that the already-inflamed state of the brain is not inflamed further as a result of MIA. These data suggest a complex interaction between IL-6 and other cytokines, the expressions of which are equally important in the brain response to MIA.

In addition, higher levels of ChAT activity were measured in the E16.5 BFs of both the control and poly(I:C) groups in the KOs than in either the control or poly(I:C) groups in WT mice. Furthermore, at this age, lower levels of GAD65 mRNA were detected in both control and poly(I:C) IL-6 KOs. Levels were similar to those of the poly(I:C)-treated WT mice and were significantly lower than those of WT controls. These data are consistent with the notion that there is a heightened inflammatory state in the IL-6 KO embryonic brains that is accompanied by higher ChAT activity and lower GAD65 expression.

Taken together, these observations suggest a role for IL-6 in the orchestration of cytokine and chemokine expression in the brain. They point to a role for IL-6 in the activation of microglia, specifically in the regulation of their output of cytokines and chemokines in response to inflammation. Moreover, in the absence of IL-6, an appropriate response to inflammation is impaired. These data imply a normal role for IL-6 as a "shut-off" switch—a way to turn off excessive proinflammatory signaling and regulate the inflammatory environment. This regulation is missing in the IL-6 KO mice.

Others have shown dysregulation and neuroanatomical anomalies in the developing brain following MIA. We now add to this literature, suggesting that MIA also has transient, but robust, effects on cholinergic development in the BF.

METHODS

Animals

C57BL/6J mice and transgenic strains were purchased from the Jackson Laboratory (Bar Harbor, ME). Homozygous B6.129P-$Cx3cr1^{tm/Litt}$/J (Cx3cr1-GFP) mice express EGFP under the control of the promoter for the fractalkine receptor (CX3CR1). Therefore, EGFP is expressed in all cells derived from a monocytic lineage (37). B6.Cg-Tg (RP23-268L19-eGFP)2Mik/J ($ChAT^{BAC}$-EGFP) mice express both EGFP and ChAT proteins. In B6.129S2-$Il6^{tm1Kopf}$/J IL-6 knockout mice, no endogenous IL-6 is expressed.

Pregnant mice were given intraperitoneal injections of 20 mg/kg poly(I:C) (potassium salt; Sigma-Aldrich, St. Louis, MO) dissolved in 200 µl 0.9% sterile saline at E12.5. Control mice were injected with 200 µl sterile saline. All animal protocols were reviewed and approved by the Rutgers Institutional Animal Care and Use Committee.

Assessment of Sickness Behavior

Behavior of saline-injected and poly (I:C)-injected mice was assessed at 4 and 24 h following injection to distinguish between normal and "sickness" behavior according to a rubric based on published guidelines (38). Pregnant females were placed in a new cage and observed for 2 min. They were scored from 0 to 4 in each of five categories that included grooming, cage exploration, posture, activity, and reactivity to touch. A "normal" mouse would score 4 in each behavior category for a total score of 20.

ChAT Assay

ChAT activity in embryonic BF tissue was assayed as described by us previously (20) following the method of Fonnum (39). In this assay, endogenous ChAT converts ^{14}C-acetyl CoA to ^{14}C-acetylcholine, which is then counted by liquid scintillation.

Stereological Analysis

E16.5 and P1 brains from CX3CR1-EGFP and ChAT-EGFP mice were fixed (4% paraformaldehyde/0.1 mol/l phosphate-buffered saline), cryoprotected in sucrose, sectioned coronally (60 µm), and mounted and coverslipped using Vectashield Hard Set (Vector Laboratories, Burlingame, CA). Stereology was performed with an Olympus Bx51 microscope equipped with an x–y–z motorized stage and Retiga 200R digital camera (Qimaging, Surrey, British Columbia, Canada). The Optical Fractionator Probe of Stereo Investigator software (MicroBrightField, Williston, VT) was used throughout. Section

Table 1. Primers used

GABA receptor subunit α1	F: ATCCGGTTTGCGCTGGGACG R: TCTGCGTGCTCCTGCACTGG
GAD65	F: CCTATGAGATCGCCCCTGTA R: GCATGGCATACATGTTGGAG
GAD67	F: CACAAACTCAGCGGCATAGA R: CTGGAAGAGGTAGCCTGCAC
GAPDH	F: GGAGCGAGACCCCACTAACA R: ACATACTCAGCACCGGCCTC
IL-1β	F: AAATACCTGTGGCCTTGGGC R: CTTGGGATCCACACTCTCCAG
IL-6	F: TTCCATCCAGTTGCCTTCTTGG R: TTCTCATTTCCACGATTTCCCAG
IL-10	F: TGACTGGCATGAGGATCAGC R: ACTCCGCAGCTCTAGGAGCA
TNFα	F: CGTGGAACTGGCAGAAGAGG R: CTGCCACAAGCAGGAATGAG

F, forward; GABA, gamma-aminobutyric acid; GAD, glutamic acid decarboxylase; GAPDH, glyceraldehyde 3-phosphate dehydrogenase; IL, interleukin; R, reverse; TNF, tumor necrosis factor.

outlines and BF contours were drawn using brightfield microscopy at ×4. Counts were performed using a ×40 objective and GFP detection filter. The grid size was 300 μm × 325 μm, and the counting frame was set at 150 μm × 150 μm. Counting was performed in a 20 μm z-depth with 2 μm guard zones. Population estimates were weighted by section thickness. Cells were counted within the BF contour in 10 sections from each E16.5 brain and 12 sections from P1 brains. Population estimates thus represent a 600 μm and a 720 μm section of the BF respectively. The coefficient of error was <0.10.

Quantitative Real-Time PCR

Total RNA was extracted using TRIzol Reagent (Life Technologies, Carlsbad, CA). cDNA was produced from 0.5 μg of RNA using random hexamers and Moloney Murine Leukemia Virus Reverse Transcriptase (Promega, Madison, WI) and amplified using SYBR Green PCR Master Mix (Applied Biosystems, Foster City, CA) or RT^2 SYBR Green/ROX qPCR Mastermix (SA Biosciences, Germantown, MD). Primers (Integrated DNA Technologies, Coralville, IA) were designed using Primer Express (Applied Biosystems) or Primer-Blast (http://www.ncbi.nlm.nih.gov). Primers are listed in **Table 1**. qRT-PCR was performed using the ABI Prism 7900HT Sequence Detection System (Applied Biosystems). Serially diluted standards were prepared from sample cDNA for each primer to calculate relative concentrations of target message. This was normalized to glyceraldehyde 3-phosphate dehydrogenase.

Enriched Populations of Fetal Microglia

To obtain enriched populations of fetal microglia, brains from embryos of a litter were pooled and minced. They were dissociated enzymatically (0.05% trypsin, 2 mmol/l EDTA, 20 μg/ml deoxyribonuclease I (DNase), all from Sigma-Aldrich) and mechanically (using the gentleMACS dissociator; Miltenyi Biotec, Auburn, CA). Serum-containing medium with 0.5 mg/ml soybean trypsin inhibitor (Sigma-Aldrich) and 40 μg/ml DNase was added to stop the reaction. The suspension was filtered through a 40 μm cell strainer and washed. Resuspended cells were incubated with 10 μl anti-CD11b magnetic beads per 10^7 cells (Miltenyi Biotec) according to manufacturer's instructions and separated using an autoMACS magnetic cell sorter (Miltenyi Biotec). Positive and negative fractions were retained for downstream assays. A 200 μl sample of each fraction was placed on a microscope slide and coverslipped. Ten fields of view were counted to determine the proportion of GFP+ cells present in the fraction because they would represent the microglial fraction. Ten separate experiments showed that the CD11b$^+$ fraction contained 49.1 ± 5% microglia, whereas the CD11b$^-$ fraction lacked any detectable microglia.

Table 2. Cytokines and chemokines in the Luminex assay

Cytokines	Chemokines
IL-1α	Eotaxin (CCL11)
IL-1β	IFNγ-induced protein 10 (IP-10; CXCL10)
IL-2	KC (CXCL1)
IL-3	LIX (CXCL5)
IL-4	Monocyte chemotactic protein 1 (MCP-1; CCL2)
IL-5	Monokine induced by gamma interferon (MIG; CXCL9)
IL-6	Macrophage inflammatory protein 1α (MIP-1α; CCL3)
IL-7	MIP-1β (CCL4)
IL-9	MIP2 (CXCL2)
IL-10	Regulated and normal T cell expressed and secreted (RANTES; CCL5)
IL-12p40	
IL-12p70	
IL-13	
IL-15	
IL-17	
Interferon-γ (IFNγ)	
Tumor necrosis factor-α (TNFα)	
Leukemia inhibitory factor (LIF)	
Granulocyte colony-stimulating factor (G-CSF)	
Granulocyte/monocyte colony-stimulating factor (GM-CSF)	
Monocyte colony-stimulating factor (M-CSF)	
Vascular endothelial growth factor (VEGF)	

IL, interleukin; KC, keratinocyte chemoattractant; LIX, lipopolysaccharide-induced CXC chemokine.

Luminex Assay

Protein was extracted from cells of the CD11b$^+$ and CD11b$^-$ fractions using Tissue Extraction Reagent I (Life Technologies, Grand Island, NY) and a proteinase inhibitor cocktail (Sigma-Aldrich). Mouse 32-plex Cytokine/Chemokine Luminex assays (EMD Millipore) were performed by Robert Donnelly (The New Jersey School of Medicine, University of Medicine and Dentistry of New Jersey). Samples and standards were run in duplicate. Results were normalized to protein concentration of samples. Cytokines and chemokines examined are listed in **Table 2**.

Statistical Analyses

Statistical analyses were performed using SigmaStat (SyStat, San Jose, CA), XL-STAT (Addinsoft, New York, NY), Primer of Biostatistics (Stanton A. Glantz, McGraw-Hill, Burr Ridge, IL), and Vassarstats (Richard Lowry, Vassar College, Poughkeepsie, NY). Student's *t*-test was used to compare two groups. Data for multiple groups were compared using a one- or two-way ANOVA or an analysis of covariance followed by a *post hoc* Tukey test. Data from the Luminex assay were reported as log pg/mg of protein. Because we hypothesized that poly(I:C) treatment would only serve to elevate cytokines (except IL-10), a one sample, one-tailed *t*-test was used to compare the differences between the log-transformed values. A P value of <0.05 was considered significant.

STATEMENT OF FINANCIAL SUPPORT

This work was supported by grants to G.M.J. and N.M.P. from Autism Speaks and the New Jersey Governor's Council for Medical Research and Treatment of Autism.

Disclosure: We have no financial disclosures to make.

REFERENCES

1. Wang K, Zhang H, Ma D, et al. Common genetic variants on 5p14.1 associate with autism spectrum disorders. Nature 2009;459:528–33.
2. Glessner JT, Wang K, Cai G, et al. Autism genome-wide copy number variation reveals ubiquitin and neuronal genes. Nature 2009;459:569–73.
3. Lipkin WI, Hornig M. Microbiology and immunology of autism spectrum disorders. Novartis Found Symp 2003;251:129–43; discussion 144–8, 281–97.
4. Hagberg H, Mallard C. Effect of inflammation on central nervous system development and vulnerability. Curr Opin Neurol 2005;18:117–23.
5. Macêdo DS, Araújo DP, Sampaio LR, et al. Animal models of prenatal immune challenge and their contribution to the study of schizophrenia: a systematic review. Braz J Med Biol Res 2012;45:179–86.
6. Pardo CA, Eberhart CG. The neurobiology of autism. Brain Pathol 2007;17:434–47.
7. Croonenberghs J, Bosmans E, Deboutte D, Kenis G, Maes M. Activation of the inflammatory response system in autism. Neuropsychobiology 2002;45:1–6.
8. Patterson PH. Maternal infection: window on neuroimmune interactions in fetal brain development and mental illness. Curr Opin Neurobiol 2002;12:115–8.
9. Ratnayake U, Quinn TA, Castillo-Melendez M, Dickinson H, Walker DW. Behaviour and hippocampus-specific changes in spiny mouse neonates after treatment of the mother with the viral-mimetic Poly I:C at mid-pregnancy. Brain Behav Immun 2012;26:1288–99.
10. Meyer U, Murray PJ, Urwyler A, Yee BK, Schedlowski M, Feldon J. Adult behavioral and pharmacological dysfunctions following disruption of the fetal brain balance between pro-inflammatory and IL-10-mediated anti-inflammatory signaling. Mol Psychiatry 2008;13:208–21.
11. Fatemi SH, Earle J, Kanodia R, et al. Prenatal viral infection leads to pyramidal cell atrophy and macrocephaly in adulthood: implications for genesis of autism and schizophrenia. Cell Mol Neurobiol 2002;22:25–33.
12. Rousset CI, Chalon S, Cantagrel S, et al. Maternal exposure to LPS induces hypomyelination in the internal capsule and programmed cell death in the deep gray matter in newborn rats. Pediatr Res 2006;59:428–33.
13. Shi L, Fatemi SH, Sidwell RW, Patterson PH. Maternal influenza infection causes marked behavioral and pharmacological changes in the offspring. J Neurosci 2003;23:297–302.
14. Jonakait GM. The effects of maternal inflammation on neuronal development: possible mechanisms. Int J Dev Neurosci 2007;25:415–25.
15. Vargas DL, Nascimbene C, Krishnan C, Zimmerman AW, Pardo CA. Neuroglial activation and neuroinflammation in the brain of patients with autism. Ann Neurol 2005;57:67–81.
16. Zimmerman AW, Jyonouchi H, Comi AM, et al. Cerebrospinal fluid and serum markers of inflammation in autism. Pediatr Neurol 2005;33:195–201.
17. Morgan JT, Chana G, Pardo CA, et al. Microglial activation and increased microglial density observed in the dorsolateral prefrontal cortex in autism. Biol Psychiatry 2010;68:368–76.
18. Mazzoni IE, Kenigsberg RL. Microglia from the developing rat medial septal area can affect cholinergic and GABAergic neuronal differentiation *in vitro*. Neuroscience 1997;76:147–57.
19. Jonakait GM, Luskin MB, Wei R, Tian XF, Ni L. Conditioned medium from activated microglia promotes cholinergic differentiation in the basal forebrain *in vitro*. Dev Biol 1996;177:85–95.
20. Ni L, Acevedo G, Muralidharan B, Padala N, To J, Jonakait GM. Toll-like receptor ligands and CD154 stimulate microglia to produce a factor(s) that promotes excess cholinergic differentiation in the developing rat basal forebrain: implications for neurodevelopmental disorders. Pediatr Res 2007;61:15–20.
21. Perry EK, Lee ML, Martin-Ruiz CM, et al. Cholinergic activity in autism: abnormalities in the cerebral cortex and basal forebrain. Am J Psychiatry 2001;158:1058–66.
22. Bauman ML, Kemper TL. Neuroanatomic observations of the brain in autism: a review and future directions. Int J Dev Neurosci 2005;23:183–7.
23. Cai Z, Pan ZL, Pang Y, Evans OB, Rhodes PG. Cytokine induction in fetal rat brains and brain injury in neonatal rats after maternal lipopolysaccharide administration. Pediatr Res 2000;47:64–72.
24. Liverman CS, Kaftan HA, Cui L, et al. Altered expression of pro-inflammatory and developmental genes in the fetal brain in a mouse model of maternal infection. Neurosci Lett 2006;399:220–5.
25. Kannan S, Saadani-Makki F, Muzik O, et al. Microglial activation in perinatal rabbit brain induced by intrauterine inflammation: detection with 11C-(R)-PK11195 and small-animal PET. J Nucl Med 2007;48:946–54.
26. Hutton LC, Castillo-Melendez M, Smythe GA, Walker DW. Microglial activation, macrophage infiltration, and evidence of cell death in the fetal brain after uteroplacental administration of lipopolysaccharide in sheep in late gestation. Am J Obstet Gynecol 2008;198:117.e1–11.
27. Smith SE, Li J, Garbett K, Mirnics K, Patterson PH. Maternal immune activation alters fetal brain development through interleukin-6. J Neurosci 2007;27:10695–702.
28. Lasala N, Zhou H. Effects of maternal exposure to LPS on the inflammatory response in the offspring. J Neuroimmunol 2007;189:95–101.
29. Garay PA, Hsiao EY, Patterson PH, McAllister AK. Maternal immune activation causes age- and region-specific changes in brain cytokines in offspring throughout development. Brain Behav Immun 2013;31:54–68.
30. Jonakait GM, Pratt L, Acevedo G, Ni L. Microglial regulation of cholinergic differentiation in the basal forebrain. Dev Neurobiol 2012;72:857–64.
31. Di Cristo G, Pizzorusso T, Cancedda L, Sernagor E. GABAergic circuit development and its implication for CNS disorders. Neural Plast 2011;2011:623705.
32. Wei H, Zou H, Sheikh AM, et al. IL-6 is increased in the cerebellum of autistic brain and alters neural cell adhesion, migration and synaptic formation. J Neuroinflammation 2011;8:52.
33. Samuelsson AM, Jennische E, Hansson HA, Holmäng A. Prenatal exposure to interleukin-6 results in inflammatory neurodegeneration in hippocampus with NMDA/GABA(A) dysregulation and impaired spatial learning. Am J Physiol Regul Integr Comp Physiol 2006;290:R1345–56.
34. Ashdown H, Dumont Y, Ng M, Poole S, Boksa P, Luheshi GN. The role of cytokines in mediating effects of prenatal infection on the fetus: implications for schizophrenia. Mol Psychiatry 2006;11:47–55.
35. Zaretsky MV, Alexander JM, Byrd W, Bawdon RE. Transfer of inflammatory cytokines across the placenta. Obstet Gynecol 2004;103:546–50.
36. Urakubo A, Jarskog LF, Lieberman JA, Gilmore JH. Prenatal exposure to maternal infection alters cytokine expression in the placenta, amniotic fluid, and fetal brain. Schizophr Res 2001;47:27–36.
37. Jung S, Aliberti J, Graemmel P, et al. Analysis of fractalkine receptor CX(3) CR1 function by targeted deletion and green fluorescent protein reporter gene insertion. Mol Cell Biol 2000;20:4106–14.
38. Crawley JN. What's Wrong with My Mouse? Hoboken, NJ: Wiley, 2007.
39. Fonnum F. A rapid radiochemical method for the determination of choline acetyltransferase. J Neurochem 1975;24:407–9.